INT. J. REMOTE SENSING, 1999, VOL. 20, NO. 4, 767–787

Agricultural crop monitoring using airborne multi-spectral imagery and C-band synthetic aperture radar

E. A. CLOUTIS,† D. R. CONNERY‡ and F. J. DOVER
Aero Sense, 2nd Floor, 1115A—46 Avenue S. E., Calgary, Alberta, Canada T2G 2A5

(*Received 6 May 1997; in final form 13 March 1998*)

Abstract. Airborne optical multi-spectral and C-band HH-polarized Synthetic Aperture Radar (SAR) imagery were acquired in conjunction with contemporaneous ground-based measurements of various crop conditions (Leaf Area Index, canopy temperature, plant height) at a test site in southern Alberta, Canada on July 19–20, 1994. Data were acquired for a variety of crops (wheat, canola, peas and beans) and irrigation practices. A number of crop condition–imagery relationships were examined to determine whether the imagery could be used to measure the various crop condition parameters. A number of statistically significant correlations were found between the imagery and the crop condition parameters, and these correlations vary as a function of crop type, sensor and crop condition parameter. The results suggest that airborne remote sensing is well suited for measuring variations in crop conditions and that C-band SAR and multi-spectral imagery provide complementary information.

1. Introduction

In order to investigate the potential applications of high spectral resolution optical remote sensing and C-band SAR imagery to agricultural crop condition monitoring, an airborne remote sensing campaign was undertaken for a number of quarter-section test sites in southern Alberta (one quarter-section is equivalent to 160 acres or 64.7 ha). The goals of the project included investigating whether these types of imagery are capable of detecting variations in crop condition parameters such as Leaf Area Index (LAI), plant height (PH), and normalized canopy temperatures (CT), which may be indicative of crop health, and how the results of the combined SAR–optical imagery compare with the individual sensor results.

Applications of airborne multi-spectral optical remote sensing to crop condition monitoring have been undertaken by a number of investigators (e.g. Stutte *et al.* 1990, Wallace *et al.* 1993, Fernández *et al.* 1994). The results of these and other studies of the optical spectral responses of stressed vegetation have been somewhat mixed. The spectral effects due to various stress-causing agents are not the same in all cases and some studies have found that normal plant spectral variations may be more significant than stress-induced variations (Tingle and Stoll 1990, Cohen 1991).

†Now at Golder Associates, Calgary, Alberta, Canada.
‡Now at the University of Winnipeg, Winnipeg, Manitoba, Canada.

International Journal of Remote Sensing
ISSN 0143-1161 print/ISSN 1366-5901 online
http://www.tandf.co.uk/JNLS/res.htm
http://www.taylorandfrancis.com/JNLS/res.htm

In addition, simple spectral indices, such as red edge derivatives, may be affected by a larger number of factors than previously believed (Banninger 1989, Boochs *et al.* 1990, Railyan and Korobov 1993).

The vast majority of previous studies involving SAR applications to agriculture have focused on the effects on radar backscatter of different canopy architectures (e.g. Ulaby and Wilson 1985, Bouman and van Kasteren 1990b), incidence angles (e.g. Daughtry *et al.* 1991), radar wavelength (e.g. Thomson *et al.* 1990, Brown *et al.* 1992), soil moisture variations (e.g. Pultz *et al.* 1990, Fischer *et al.* 1992), surface roughness (e.g. Hutton and Brown 1986, Boivin *et al.* 1990, Major *et al.* 1993), and crop types (e.g. Pultz and Brown 1987, Treitz *et al.* 1991, Foody *et al.* 1994).

Applications of synthetic aperture radar data to monitoring variations in crop characteristics have been limited. Brisco and Brown (1990) examined the applications of airborne C-HH SAR data to drought stress detection for various crops in southern Saskatchewan. The analysis involved two classes of drought stress (poor/good) for four crop types as well as water and summer fallow classes. It was found that the degree of separability was quite variable and some classes were only poorly discriminated. Average backscatter was found to be higher for the healthier crops. Major *et al.* (1991) measured radar backscatter from canola and wheat canopies and found that good statistical relationships existed between radar backscatter and volumetric canopy moisture (positively correlated). Prevot *et al.* (1993) examined the applications of multi-frequency, polarization, and incidence angle SAR data for monitoring wheat canopies. The data were used to develop an algorithm to estimate vegetation water content from SAR data acquired at two different incidence angles.

Few studies have investigated the complementarity of optical–SAR imagery for agricultural applications. Brisco *et al.* (1989) used combined Landsat TM and airborne SAR data for early season crop discrimination in southern Saskatchewan. They found that crop discrimination improved as the number of channels used in the analysis increased. A similar study by Dixon and Mack (1991) also found that combined optical–SAR imagery yielded the highest crop discrimination accuracy. A multi-temporal study by Brisco and Brown (1995) found that combined Landsat TM and SAR data could be used successfully for crop type classification and that there was a temporal dependence on crop type discrimination. Smith *et al.* (1995) have applied a variety of optical and SAR data sets to soil conservation and management monitoring. In a more general study, Paris and Kwong (1988) found that combined Landsat TM and SIR-B SAR could be used to derive various vegetation parameters such as green LAI and percent ground cover.

The results of these and other studies suggest that combined optical and SAR data could be successfully applied to detecting relative variations in crop characteristics within a single field. The program whose results are detailed below was designed to acquire high spectral resolution optical and SAR imagery for a number of agricultural crops in conjunction with ground-based measurements of crop conditions (LAI, PH and canopy temperatures) which may be indicative of crop health. The goal is to determine which parameters can be derived from the airborne imagery and whether the relationships between the imagery and ground-based indicators of crop condition vary as a function of crop type and sensor.

This study is a continuation of earlier work which examined the applications of optical remote sensing and synthetic aperture radar imagery to this same task (Cloutis *et al.,* 1996a, b). In these studies it was found that optical data can, in many cases, provide statistically significant measures of crop condition parameters for a variety of crops. Similarly, various types of SAR images were also found to be correlated with crop condition parameters. In both cases the statistically significant correlations found varied as a function of number of bands or images used in the analysis, crop type, time of year and crop condition parameter. The purpose of this paper is to extend this analysis to looking at the level of statistical significance of optical + SAR data for measuring these same crop condition parameters.

2. Study area

The project involved the acquisition and analysis of ground-based and airborne optical multi-spectral and C-band HH-polarized SAR data. A study area was identified near the town of Lomond, Alberta, consisting of nine quarter-sections (64.7 ha each) planted with a variety of crops and with variable irrigation practices (figure 1). These fields were subjected to detailed investigation on July 19–20, 1994. The nature of these fields is provided in table 1. Crops which were involved in the study included wheat, wheat underseeded to alfalfa, beans, peas and canola (a broadleaf oilseed crop), irrigated using central pivot and line irrigation as well as dryland farming. Ground-based data were acquired while the fields were in different stages of irrigation. This provided a more heterogeneous data set than would otherwise have been the case.

The results of separate analysis of the airborne multi-spectral sensor and airborne synthetic aperture radar have been presented elsewhere (Cloutis *et al.* 1996a, b).

3. Data collection and processing

The airborne campaign was preceded by a laboratory component designed to investigate the spectrum-altering effects on various crops of different stress-causing agents. This study was undertaken because it was felt that variations in crop conditions in the field could be attributed to various stress-causing agents such as soil salinity or underwatering/overwatering. This information was supplemented by the results of previous investigations. The available data suggested that spectral parameters could not be used to distinguish between different stress-causing agents (Carter *et al.* 1992, Carter 1993, 1994). In addition it was found that narrow spectral bands were better suited for crop stress discrimination than broad bands (Demetriades-Shah *et al.* 1990, Stutte *et al.* 1990, Carter 1994, Peñuelas *et al.* 1994). A set of 13 narrow wavelength bands was selected for their application to crop stress detection on the basis of the available information. This band set was termed the enhanced geobotany (EG) band set (table 2). Bands 1–5 are located in the visible spectral region, bands 6–9 are located in a region of abrupt change in reflectance, hereafter referred to as the 'red edge', and bands 10–13 are located in a region of relatively constant reflectance, hereafter referred to as the 'NIR reflectance plateau'.

The study area was overflown on July 19, 1994 by the Aero Sense twin engine Cessna 340 aircraft equipped with the Compact Airborne Spectrographic Imager (*casi*) (Anger *et al.* 1994). Data were collected in spatial mode, resulting in full coverage for the 13 spectral bands of the EG band set (table 2). The area was overflown at 3970 m above ground level, resulting in average spatial resolution of 5 m (across and along track). The *casi* instrument collects 512 pixels across track, resulting in a swath width of ~2.5 km. The aircraft was equipped with a GPS receiver and gyroscope, allowing the imagery to be corrected for aircraft-induced distortions.

The study area was also overflown on this date by the Canada Centre for Remote

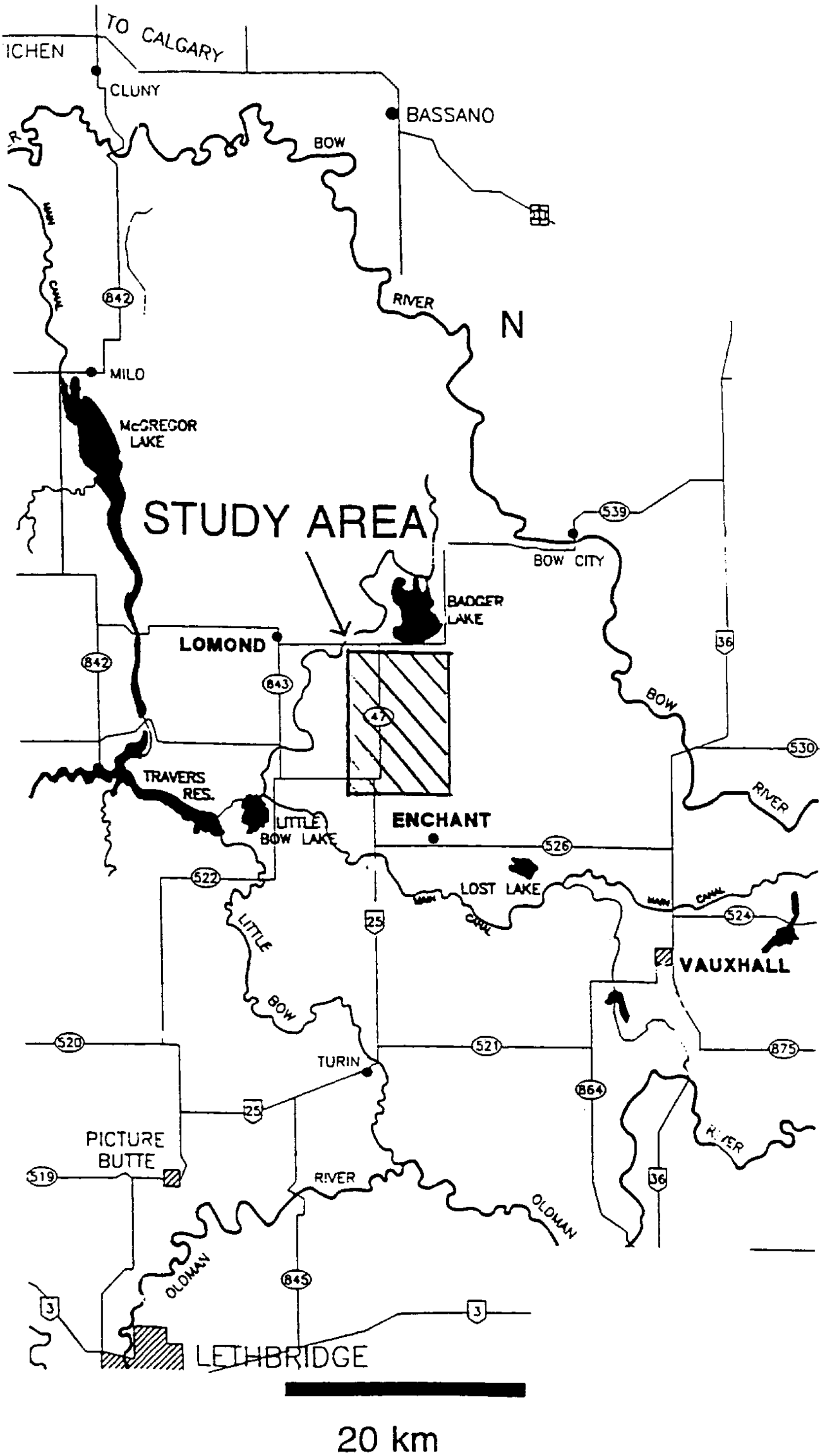

Figure 1. Location of study area near the town of Lomond in the southern part of the province of Alberta, Canada (the study area is centred at 112° 30′ 00″ W and 50° 15′ 15″ N).

Table 1. Characteristics of the sampled quarter-sections near Lomond, Alberta, Canada.

Quarter-section	Crop type and extent	Irrigation method
SW 05-15-18	Wheat (40.5 ha eastern portion and dry corners) Peas (24.3 ha western portion)	Central pivot
NW 24-15-19	Wheat (64.7 ha)	Central pivot
NE 25-15-19	Canola (52.6 ha irrigated portion) Summer fallow (6.1 ha northern two dry corners) Wheat underseeded to grass (6.1 ha 2 southern dry corners)	Central pivot
NE 26-15-19	Wheat underseeded to alfalfa (64.7 ha)	Central pivot
NW 26-15-19	Peas (28.3 ha northern half of irrigated portion) Canola (28.3 ha southern half of irrigated portion) Wheat (8.1 ha dry corners)	Central pivot
SE 26-15-19	Wheat (64.7 ha)	Line irrigation
SW 26-15-19	Wheat (32.4 ha) Summer fallow (32.4 ha)	None
NE 27-15-19	Wheat (52.6 ha irrigated part and two eastern dry corners) Summer fallow (12.1 ha two western dry corners)	Central pivot
SE 27-15-19	Beans (52.6 ha irrigated portion) Summer fallow (12.1 ha dry corners)	Central pivot

Table 2. Enhanced geobotany band set parameters and SAR images used in the analysis.

(a) Geobotany band set

Band	Wavelength interval (nm)	Band centre (nm)	Width (nm)	Spectral region
1	474.7–501.1	487.9	26.4	Visible
2	526.3–536.3	531.3	10.0	
3	546.9–557.5	552.2	10.6	
4	596.4–607.0	601.7	10.6	
5	655.0–665.0	660.0	10.0	Red edge
6	676.4–684.5	680.5	8.1	
7	695.0–702.0	698.5	7.0	
8	702.0–708.0	705.0	6.0	
9	708.6–715.8	712.2	7.2	
10	733.3–740.9	737.1	7.6	NIR plateau
11	744.5–751.7	784.1	7.2	
12	770.0–780.0	775.0	10.0	
13	784.1–789.5	786.8	5.4	

(b) SAR data sets

Raw image (no filtering)
3×3 filtered image
11×11 filtered image
Textural homogeneity
Textural contrast
Textural mean
11×11 filtered image + textural mean

Sensing Convair 580 aircraft equipped with a C-band synthetic aperture radar system (Livingstone *et al.* 1987). Data were acquired in the narrow mode (45–76° incidence angle) with three polarizations (HH, HV and VV); only the HH-polarized data have been used in the current analysis in order to provide data most compatible with that available from Radarsat. The study area was overflown at 4970 m above ground level, resulting in a spatial resolution of 4.8 m along track and 6.1 m across track. All of the test sites were within 5 km of each other in the across track direction, consequently backscatter variation was assumed to be indicative of surface variation rather than incidence angle effects. The difference in incidence angle across the study area was on the order of 5° (~50–55°).

A number of radar 'images' were used in the analysis, including the antenna pattern corrected image and tonal images generated using 3×3 and 11×11 pixel size Frost adaptive filters. PCI EASI/PACE software was used for filtering as well as for generating various measures of textural variations, including textural mean, homogeneity, contrast, and entropy (table 2). These textural measures were chosen because they are easily calculated using PCI software and the two extremes in filter sizes were selected in order to be able to quickly gauge the effects of large changes in filter size. Because of the large volume of data that was generated, only selected results can be presented here. The ensuing discussion focuses on the filtered and unfiltered tonal radar images and the textural mean.

The *casi* imagery of the study area consisted of four flight lines. The flight lines for which GPS and gyroscope data were available were corrected for aircraft roll, pitch and yaw by Itres Research Ltd using proprietary software. For the flight lines which did not include GPS information, gyroscope information was used to correct for aircraft roll. Radiometric correction of the imagery was performed by scaling the data to occupy the full eight-bit dynamic range, i.e. DN values range from 0 to 255. This procedure was used to provide a consistent method for calibration of all of the flight lines in the absence of detailed atmospheric profiles required for full radiometric correction.

The radar and *casi* imagery were integrated for analysis using PCI EASI/PACE software (PCI 1992). Registration errors were on the order of 1–2 pixels. Ground-based sample locations were located in the geocorrected imagery. The spectral and radar backscatter values for 2×2 pixel blocks at each of the sample locations were extracted from the imagery and averaged in order to provide greater assurance that each sample location was included in the analysis. During registration the SAR data were resampled to *casi* resolution.

Both irrigated (central pivot and line irrigated) and unirrigated fields were included in the study (table 1). Sampling locations were generally situated at the intersection of pivot wheel tracks with diagonal field transects. These locations were also paced off to provide an additional check on location. Sample locations in fields without central pivot irrigation were selected by pacing alone. The repeatability of these locations was on the order of 5 m. Sample locations were generally spaced approximately 50 m apart and transects were generally oriented from one corner of a quarter-section towards the central pivot. Transects in the other fields were based on readily identifiable landmarks, both natural and anthropogenic. Ground-based measurements were conducted contemporaneously with the overflights and extended into the following day (July 19–20).

Ground-based crop data that were collected included average plant height (PH), canopy minus ambient air temperature (CT), and Leaf Area Index (LAI). Multiple readings were taken at each sample location in the field and averaged for each station. Data were collected within 5 m of the central sample location. Air temperatures were measured with a sling psychrometer at the beginning and end of each field transect and interpolated for the various sample sites. Canopy temperatures were acquired with an Everest Interscience Model 110 infrared thermometer equipped with a 3° field of vision (FOV). Five measurements were taken at each sample location and averaged. The measurements were taken of sunlit leaves at a 45° zenith angle in the principal plane of the Sun. The canopy (T_c) minus ambient air temperature (T_a) were used in the analysis (T_c-T_a) and are referred to simply as canopy temperature (CT). The LAI measurements were acquired using a LiCor LAI2000 Plant Canopy Analyzer. Twelve readings were acquired at each sample site and averaged. The number of sample locations visited in each field on the three dates are listed in tables 3–6.

4. Data analysis

The spatial resolution of the airborne imagery was such that central pivot irrigation wheel tracks could not always be identified in the images. In these cases the spacing between pivot tracks as measured during the transects was used to identify the sample locations in the imagery. As the intent was to extract spectral values from the imagery corresponding to the ground-based sample locations, the locations of the ground-based stations were located on the geocorrected imagery. In order to ensure that the corresponding spectral values for each ground-based sample location were properly acquired, and given the uncertainties in precisely locating all of the sample locations in the imagery and the slight uncertainties in image registration, it was decided to extract average spectral values for a 2 × 2 pixel block at each of the sample locations. The ranges of ground-based crop conditions measured on July 19–20 are provided in table 3.

The available *casi* data included the full 13 band EG band set (table 2). The airborne spectra were used to generate a number of ratios, indices and more restricted

Table 3. Range of ground-based crop condition parameters.

Crop	Ground-based parameter	Measured range
Wheat	LAI	0.6–4.9
	T_c-T_a (°C)	− 2.7–+2.0
	PH (cm)	35–135
Canola	LAI	1.2–5.5
	T_c-T_a (°C)	− 4.0–+2.0
	PH (cm)	50–107
Beans	LAI	0.9–2.0
	T_c-T_a (°C)	− 2.4–0.7
	PH (cm)	25–35
Peas	LAI	2.8–6.1
	T_c-T_a (°C)	− 1.7–+0.6
	PH (cm)	50–70
Wheat/alfalfa	LAI	1.8–3.7
	T_c-T_a (°C)	− 1.8–+0.3
	PH (cm)	60–85

LAI = Leaf Area Index; T_c-T_a (°C) = canopy minus ambient air temperature; PH = plant height.

band sets. Carter (1994) found that the most useful ratios for detecting plant stress are the 695 nm/420 nm (Carter 1) and 695 nm/760 nm (Carter 2) reflectance ratios; given the limited short wavelength coverage of the *casi* instrument, the reflectance at 488 nm was used for the former ratio. The various band sets, ratios and indices used in the analysis are provided in table 4. The number of data points available for analysis as a function of crop type, crop condition parameter and sampling date are provided individually for each crop in the second row of tables 6–10.

The ground-based data and extracted airborne values were subjected to statistical analysis using univariate and multivariate linear regression analysis as a function of crop type. This approach is useful for determining whether variations in crop conditions which may be indicative of incipient stress (canopy temperatures) and established stress (plant height, LAI) can be deduced from the airborne imagery. Correlation coefficients were calculated for the individual *casi* bands and SAR images, as well as the various ratios and indices, and combinations of *casi* bands and/or SAR images (see tables 2 and 4).

Correlation coefficients (r) generated for individual *casi* bands, ratios and indices, and individual SAR images, can vary between -1 and $+1$; a correlation of $+1$ indicates a perfect direct relationship between two variables (in this case a *casi* band, ratio or index, or SAR image and a crop condition parameter); a correlation of -1 indicates that one variable changes inversely with relation to the other. Correlation coefficients between the two extremes indicate a less than perfect linear relationship. A correlation coefficient of zero indicates the complete lack of a linear relationship (Davis 1986). Coefficients of multiple correlation (R) were generated in the analyses involving the various band sets and combinations of the *casi* and/or SAR images (tables 2 and 4). Coefficients of multiple correlation can vary between 0 and $+1$, with the latter indicating a perfect direct relationship, and the former indicating a complete lack of a direct linear relationship.

The statistical significance of the various crop condition-spectral correlations was also assessed. The Student t-test was used for determining the level of statistical significance of the derived correlation coefficients. These coefficients were assessed at the 99% level of significance, corresponding to $\sim 2.6\,\sigma$ (Davis 1986). In the ensuing discussion, statistically significant is used to indicate that the correlation coefficients

Table 4. Spectral parameters used in the analysis.

Parameter	Description based on enhanced geobotany bands (table 2)
Ratios and indices	
Casi NDVI	((EG12 + EG13) − (EG5 + EG6))/((EG12 + EG13) + (EG5 + EG6))
Casi TM4/3	(EG12 + EG13)/(EG5 + EG6)
Carter 1	EG7/EG1
Carter 2	EG7/EG12
IR/Red	EG13/EG6
Red edge 1	EG9/EG6
Red edge 2	(EG9-EG6)/(EG9 + EG6)
Band sets	
Geobotany band set	EG1, EG3, EG4, EG6, EG9, EG10, EG11, EG13
Red edge band set	EG5, EG6, EG7, EG8, EG9, EG10
Botany band set	EG3, EG6, EG9, EG13

are significant at this level. As statistical significance is a function of the number of degrees of freedom, the correlation coefficients based on the band sets and combinations of bands/images will generally be higher than for the individual bands, but this difference may not be statistically significant. In addition, some crop condition parameter data sets contained insufficient points to yield correlation coefficients. Correlation coefficients which are statistically robust at the 99% level are highlighted in the data tables for each crop. As the degrees of freedom decrease, either due to a reduction in the number of data points, or an increase in the number of bands used in the analysis, progressively higher correlation coefficients are required for a given level of statistical significance.

Given the large number of permutations and combinations involving 13 *casi* bands, ratios and indices, and 7 SAR images, it is not possible to discuss or present all of the results. Consequently the ensuing discussion focuses on the issue of complementarity of the *casi* and SAR imagery. Analysis focused on only four of the seven SAR images: the APC and two Frost filter images (in order to examine the effects of filter size variations), and the textural mean image. The latter was chosen because it generally provided the highest correlation coefficients, both singly (Cloutis *et al.* 1996b) and in combination with the optical data; thus the maximum improvement in correlation with the inclusion of textural data could be evaluated. Our selection of *casi* bands was based on our desire to include bands across the full spectral range of the *casi* instrument rather than basing our selection on adjacent band correlations.

The full range of optical multi-spectral bands, ratios and indices used in the analysis can be grouped together for comparative purposes. As mentioned, EG bands 1–5 are located in the visible spectral region and previous investigators have found that visible region plant spectra often exhibit variations due to various stress-causing agents (Carter 1993, Carter and Miller 1994). EG bands 6–9 are located along the so-called vegetation 'red edge', a region of rapidly increasing reflectance in plant spectra which often, but not always, exhibits systematic variations due to various stress-causing agents (Boochs *et al.* 1990, Railyan and Korobov 1993). EG bands 10–13 are located in the near infrared region along the so-called vegetation 'reflectance plateau', which is generally characterized by high overall reflectance for healthy plants and often exhibits variations due to various stress-causing agents (Miller *et al.* 1990, Malthus and Madeira 1993, Peñuelas *et al.* 1994). Thus it is expected that spectral variations in these wavelength regions could be correlated with variations in crop stress.

Of the various indices and ratios used in the analysis, the Carter 1 and 2, *casi* NDVI and TM4/3 and IR/Red parameters involve bands from at least two of the band groupings cited above. The Red Edge 1 and 2 parameters involve bands exclusively from the 'red edge' region and hence are useful for determining whether systematic variations in red edge reflectance exist. The various band combinations (botany, red edge, geobotany, and enhanced geobotany) are useful for assessing the number and nature of bands which are necessary for measuring variations in the various crop condition parameters for a given crop and level of statistical significance.

The possibility of collinearity problems is inherent in the acquisition of hyperspectral data. This involves the possibility that some bands (adjacent bands being the likeliest candidates) may respond in essentially the same manner to variations in crop condition parameters. This collinearity will not be apparent in the correlation coefficients generated, but its presence would reduce the robustness of the data.

In order to examine the seriousness of this issue, correlation coefficient matrices were generated for the 13 *casi* bands. In this way, the presence of high correlation coefficients could be immediately identified. While a rigorous analysis of the collinearity of the *casi* bands is beyond the scope of this paper, the issue of collinearity must be addressed. Table 5 presents the range of correlation coefficients between adjacent *casi* bands as a function of crop type. The results indicate that a range of colinearities exist between adjacent *casi* bands, as well as the fact that a number of bands do not exhibit significant colinearities. It should however be noted use of the term 'adjacent' *casi* bands is a bit of a misnomer as the *casi* bands in the enhanced geobotany band set are not directly adjacent to each other, with the exception of bands 7, 8 and 9. Adjacent in the case of the other bands refers to those bands that are closest to each other in wavelength space.

5. Results

For the purposes of analysis, each crop is discussed individually. In addition, the discussion is restricted to the same bands and band combinations for each crop. This approach allows variations as a function of crop type to be highlighted. The results for individual *casi* bands and the radar imagery have been presented elsewhere (Cloutis *et al.* 1996a, b). Briefly it was found that SAR tonal images generally provide higher correlations to crop condition parameters than textural data, and that modest improvements in correlation are possible when both tonal and textural SAR data are included in the analysis. The examination of the optical data revealed that correlation coefficients increase with increasing number of optical bands. However both the SAR and optical data failed to provide a single image parameter which provided the highest correlation across all crop types, dates and crop condition parameters.

5.1. *Wheat*

The ground-based data collection campaigns collected the largest volumes of data for the wheat crop. The linear correlation coefficients for the wheat fields are presented in table 6. The correlation coefficients with a statistical significance exceeding 99% ($\sim 2.6\sigma$) are highlighted. With only two exceptions, the derived correlation coefficients are statistically significant at the 99% level. Not enough data points were collected from unirrigated wheat fields to enable a comparison to be made between irrigated and unirrigated fields.

The complementarity of the SAR and optical data can best be assessed by comparing the correlation coefficients for individual indices and ratios with the various combinations. In almost all cases, inclusion of tonal radar information in the analysis results in increases in correlation coefficients for all three crop parameters. The amount of increase is generally a function of the initial correlation

Table 5. Range of correlation (r) for adjacent *casi* bands in enhanced geobotany band set.

Crop	Range of correlation coefficients
Wheat	0.17–0.99
Canola	0.47–0.99
Beans	0.93–0.99
Peas	0.34–0.99
Wheat/alfalfa	0.13–0.99

Table 6. Linear correlation coefficients for wheat fields.

Casi/SAR band n[d]	LAI[a] 57	T°C[b] 32	PH[c] 43
R1	– 0.59	0.54	– 0.30
R2	– 0.63	0.59	– 0.35
R3	– 0.69	0.61	– 0.42
R4	– 0.63	0.55	– 0.31
R3 + R4	0.69	0.62	0.42
Casi NDVI	0.72	– 0.71	0.70
Casi NDVI + R3	0.80	0.73	0.76
Casi NDVI + R3 + R4	0.80	0.73	0.76
Casi NDVI + R2	0.78	0.73	0.74
Casi NDVI + R2 + R4	0.78	0.73	0.77
Casi NDVI + R1	0.77	0.72	0.73
Casi NDVI + R1 + R4	0.78	0.72	0.73
Red edge1	0.64	– 0.60	0.80
Red edge1 + R3	0.78	0.67	0.82
Red edge1 + R3 + R4	0.78	0.67	0.83
Carter 1	– 0.61	0.46	– 0.76
Carter 1 + R3	0.74	0.62	0.80
Carter 1 + R3 + R4	0.74	0.62	0.80
Carter 2	– 0.66	0.70	– 0.78
Carter 2 + R3	0.78	0.72	0.83
Carter 2 + R3 + R4	0.78	0.72	0.83
Botany	0.75	0.76	0.77
Botany + R3	0.81	0.85	0.78
Botany + R3 + R4	0.81	0.89	0.79
Geobotany	0.79	0.77	0.78
Geobotany + R3	0.86	0.87	0.79
Geobotany + R3 + R4	0.86	0.90	0.79
Enhanced geobotany	0.80	0.86	0.84
Enhanced geobotany + R3	0.87	0.93	0.84
Enhanced geobotany + R3 + R4	0.87	0.93	0.85

[a]Leaf Area Index; [b]canopy minus ambient temperature; [c]plant height; [d]number of data points used in the analysis; ND= not determined. R1= Antenna pattern corrected SAR image; R2= 3 × 3 pixel size Frost adaptive filtered SAR image; R3= 11 × 11 pixel size Frost adaptive filtered SAR image; R4= textural mean of SAR image. Correlation coefficients that are statistically significant at the 99% level are underlined.

coefficient; the lowest correlation coefficients generally exhibit the largest absolute increases when tonal radar data are included in the analysis and *vice versa* (e.g. Carter 1 index).

The various optical band combinations generally exhibit higher correlation coefficients than the ratios and indices. Even in these cases, where correlation coefficients exceed 85%, inclusion of tonal radar data results in increases in correlation coefficients.

The effect of filter size on the correlation coefficients for the SAR imagery can also be assessed from table 6. The data indicate that, as the filter size is increased, correlation coefficients increase somewhat. This effect is probably related to the scale of heterogeneities in the crop and our interpretation of this effect is discussed in an earlier paper (Cloutis *et al.* 1996b). This effect is also apparent in the combined optical–SAR data. The combinations of *casi* NDVI and the various tonal images exhibit increases in correlation coefficient as the filter size increases.

Inclusion of the textural radar data, in the form of textural mean, has little or no effect on correlation coefficients, regardless of the absolute value of the correlation coefficient. This suggests that, at least for the wheat crop, the inclusion of textural SAR information will not significantly improve the correlation accuracies.

5.2. *Canola*

The inclusion of canola fields in the analysis (table 7) allows a comparison of the results for a cereal crop (wheat) with a broad leaf crop. As this crop was less intensively sampled than the wheat crop, fewer statistically significant correlation coefficients are present. The greatest number of statistically significant correlations were found for LAI. These data exhibit a number of similarities and differences as

Table 7. Linear correlation coefficients for canola fields.

Casi/SAR band n[d]	LAI[a] 11	T °C[b] 11	PH[c] 11
R1	0.65	– 0.52	0.73
R2	0.53	– 0.45	0.60
R3	0.38	– 0.26	0.41
R4	0.49	– 0.40	0.55
R3+ R4	0.50	0.40	0.55
Casi NDVI	0.43	– 0.09	0.09
Casi NDVI+ R3	0.73	0.33	0.48
Casi NDVI+ R3+ R4	0.80	0.45	0.61
Casi NDVI+ R2	0.80	0.51	0.66
Casi NDVI+ R2+ R4	0.80	0.51	0.66
Casi NDVI+ R1	0.80	0.54	0.74
Casi NDVI+ R1+ R4	0.81	0.54	0.74
Red edge1	0.50	– 0.14	0.09
Red edge1+ R3	0.74	0.34	0.46
Red edge1+ R3+ R4	0.81	0.46	0.59
Carter 1	– 0.60	0.69	– 0.55
Carter 1+ R3	0.64	0.54	0.56
Carter 1+ R3+ R4	0.64	0.54	0.59
Carter 2	– 0.80	0.77	– 0.73
Carter 2+ R3	0.80	0.80	0.77
Carter 2+ R3+ R4	0.87	0.81	0.78
Botany	0.89	0.74	0.85
Botany+ R3	0.88	0.84	0.85
Botany+ R3+ R4	0.90	0.94	0.89
Geobotany	0.96	0.87	0.97
Geobotany+ R3	0.99	0.99	0.99
Geobotany+ R3+ R4	ND	ND	ND
Enhanced geobotany	ND	ND	ND
Enhanced geobotany+ R3	ND	ND	ND
Enhanced geobotany+ R3+ R4	ND	ND	ND

[a]Leaf Area Index; [b]canopy minus ambient temperature; [c]plant height; [d]number of data points used in the analysis; ND= not determined. R1= Antenna pattern corrected SAR image; R2= 3 × 3 pixel size Frost adaptive filtered SAR image; R3= 11 × 11 pixel size Frost adaptive filtered SAR image; R4= textural mean of SAR image. Correlation coefficients that are statistically significant at the 99% level are underlined.

compared to the wheat crop results. Unlike the wheat crop, increasing the size of the Frost adaptive filter results in decreases in correlation coefficients for the SAR data.

Once again, inclusion of radar data in the analysis generally results in increases in correlation coefficients, many of which are statistically significant, and the amount of increase is greatest for the lowest correlation coefficients. Unlike the wheat crop, however, the inclusion of the SAR textural mean generally results in increases in correlation coefficients.

The various optical band sets generally exhibit higher correlation coefficients than the ratios and indices, similar to the results for the wheat crop. Statistically significant correlation coefficients for the various band combinations can range as high as 99%, suggesting that combined optical–SAR imagery are capable of yielding quantitative information concerning various crop parameters.

5.3. *Beans*

Analysis of the results for the bean field used in this study represents something of a challenge. Since the area under bean cultivation was fully irrigated, dryland data were not available and hence the range of crop conditions was not as extensive as for the other crops (table 3). The number of ground-based measurements was quite variable, resulting in less systematic and statistically significant results than for most of the other crops examined (table 8).

The inclusion of tonal SAR data in the analysis results in increases in correlation coefficients. Like the canola crop, inclusion of SAR textural mean also results in increases in correlation coefficients, even when the coefficients exceed 85%. The data indicate that combined optical and SAR data may yield linear correlation coefficients that exceed 85%.

5.4. *Peas*

Two pea fields were sampled during the course of the campaign, allowing a more robust comparison than for a single field. In the course of the field transects it was noted that the crop exhibited wide variability in terms of visual crop health, in spite of the fact that the pea crops in both fields were fully irrigated. The greatest number of statistically significant results were obtained for LAI; the results are presented in table 9.

The radar data for the pea fields provide the highest correlation coefficients of any of the crops examined, exceeding 85% in the case of LAI. Inclusion of the SAR textural mean results in slight increases in correlation coefficients over the values obtained using optical + SAR tonal information alone. The optical band sets once again generally provide higher correlation coefficients than the optical ratios and indices. Statistically significant correlation coefficients exceeding 85% were found for all three crop parameters and a number of band/image combinations.

5.5. *Wheat underseeded to alfalfa*

Analysis of the wheat underseeded to alfalfa field presents difficulties not existing in the fields sown with a single crop. Plant height determinations are complicated by the presence of two crops (wheat heights alone were used in the analysis), while leaf area index and canopy temperature measurements are more straightforward.

The correlation coefficients for the wheat/alfalfa field are presented in table 10. The presence of two crops may account for the general lack of statistically significant

Table 8. Linear correlation coefficients for bean fields.

Casi/SAR band n[d]	LAI[a] 12	T°C[b] 5	PH[c] 22
R1	0.37	– 0.92	– 0.07
R2	0.48	– 0.89	– 0.18
R3	0.65	– 0.89	– 0.27
R4	0.43	– 0.84	– 0.08
R3 + R4	0.66	0.91	0.31
Casi NDVI	0.41	– 0.43	0.17
Casi NDVI + R3	0.70	0.89	0.35
Casi NDVI + R3 + R4	0.70	0.92	0.38
Casi NDVI + R2	0.59	0.90	0.27
Casi NDVI + R2 + R4	0.62	0.98	0.48
Casi NDVI + R1	0.54	0.92	0.19
Casi NDVI + R1 + R4	0.56	0.99	0.21
Red edge1	0.43	0.39	<u>0.59</u>
Red edge1 + R3	0.71	0.96	<u>0.64</u>
Red edge1 + R3 + R4	0.71	0.99	<u>0.67</u>
Carter 1	– <u>0.74</u>	0.85	0.32
Carter 1 + R3	<u>0.79</u>	0.92	0.33
Carter 1 + R3 + R4	<u>0.80</u>	0.93	0.37
Carter 2	– 0.47	0.45	– 0.15
Carter 2 + R3	0.71	0.89	0.34
Carter 2 + R3 + R4	0.71	0.92	0.37
Botany	<u>0.89</u>	ND	<u>0.73</u>
Botany + R3	<u>0.88</u>	ND	<u>0.74</u>
Botany + R3 + R4	<u>0.88</u>	ND	<u>0.78</u>
Geobotany	0.95	ND	<u>0.81</u>
Geobotany + R3	0.97	ND	<u>0.82</u>
Geobotany + R3 + R4	0.99	ND	<u>0.87</u>
Enhanced geobotany	ND	ND	<u>0.85</u>
Enhanced geobotany + R3	ND	ND	<u>0.85</u>
Enhanced geobotany + R3 + R4	ND	ND	<u>0.90</u>

[a]Leaf Area Index; [b]canopy minus ambient temperature; [c]plant height; [d]number of data points used in the analysis; ND = not determined. R1 = antenna pattern corrected SAR image; R2 = 3 × 3 pixel size Frost adaptive filtered SAR image; R3 = 11 × 11 pixel size Frost adaptive filtered SAR image; R4 = textural mean of SAR image. Correlation coefficients that are statistically significant at the 99% level are underlined.

correlations, particularly for LAI and canopy temperatures. Enough statistically significant results were obtained to make some general observations. The inclusion of SAR textural mean appears to result in slight increases in correlation coefficients over the optical + SAR tonal values. Correlation coefficients exceeding 95% are possible for optical + SAR data and in some cases, correlation coefficients for optical band sets + SAR data are substantially higher than those obtained using optical ratios and indices + SAR data.

6. Discussion

The results presented above suggest that the ground-based crop condition parameters which are most amenable to quantification using airborne multi-spectral imagery vary from crop to crop. Few ubiquitous trends are apparent in the data, but some general trends in the data can be discerned.

Table 9. Linear correlation coefficients for pea fields.

Casi/SAR band n[d]	LAI[a] 13	T°C[b] 7	PH[c] 7
R1	– 0.82	0.39	– 0.83
R2	– 0.89	0.33	– 0.48
R3	– 0.85	– 0.21	0.29
R4	– 0.85	0.42	– 0.73
R3+ R4	0.89	0.50	0.82
Casi NDVI	0.64	0.47	– 0.59
Casi NDVI+ R3	0.86	0.49	0.62
Casi NDVI+ R3+ R4	0.89	0.51	0.85
Casi NDVI+ R2	0.89	0.48	0.60
Casi NDVI+ R2+ R4	0.90	0.48	0.91
Casi NDVI+ R1	0.88	0.47	0.85
Casi NDVI+ R1+ R4	0.88	0.48	0.85
Red edge1	0.77	– 0.79	– 0.38
Red edge1+ R3	0.89	0.87	0.44
Red edge1+ R3+ R4	0.89	0.91	0.96
Carter 1	– 0.31	– 0.12	0.56
Carter 1+ R3	0.87	0.21	0.56
Carter 1+ R3+ R4	0.89	0.55	0.83
Carter 2	– 0.61	– 0.38	0.66
Carter 2+ R3	0.87	0.39	0.67
Carter 2+ R3+ R4	0.89	0.50	0.83
Botany	0.89	0.99	0.88
Botany+ R3	0.90	ND	ND
Botany+ R3+ R4	0.95	ND	ND
Geobotany	0.95	ND	ND
Geobotany+ R3	0.96	ND	ND
Geobotany+ R3+ R4	0.99	ND	ND
Enhanced geobotany	ND	ND	ND
Enhanced geobotany+ R3	ND	ND	ND
Enhanced geobotany+ R3+ R4	ND	ND	ND

[a]Leaf Area Index; [b]canopy minus ambient temperature; [c]plant height; [d]number of data points used in the analysis; ND= not determined. R1= antenna pattern corrected SAR image; R2= 3 × 3 pixel size Frost adaptive filtered SAR image; R3= 11 × 11 pixel size Frost adaptive filtered SAR image; R4= textural mean of SAR image. Correlation coefficients that are statistically significant at the 99% level are underlined.

It should be noted that the import of the results is a function of the statistical significance attached to them. A significance level of 99% ($\sim 2.6\,\sigma$) applied to the Student t-test was used in the current analysis. A lower level of statistical significance would have resulted in the inclusion of more correlation coefficients, albeit at a lower level of confidence.

Perhaps the most general observation that can be made is that inclusion of SAR data in the analysis results in increases in correlation coefficients across all crop types. However the particular SAR tonal image that will provide the greatest increase is not the same in all cases. The differences in the various SAR tonal images are the result of Frost adaptive filtering. The fact that filtering may result in increases or decreases in correlation coefficients may be attributable to the scale of crop variations. Fields with small-scale variations (on the order of a few metres) in crop parameters such as LAI and plant height would be most affected by filtering of SAR imagery.

Table 10. Linear correlation coefficients for wheat underseeded to alfalfa fields.

Casi/SAR band n[d]	LAI[a] 17	T°C[b] 17	PH[c] 17
R1	0.17	– 0.08	– 0.06
R2	0.15	– 0.02	0.09
R3	0.20	0.02	0.34
R4	0.24	0.11	0.03
R3 + R4	0.24	0.16	0.51
Casi NDVI	0.03	– 0.30	0.58
Casi NDVI + R3	0.20	0.31	<u>0.64</u>
Casi NDVI + R3 + R4	0.24	0.34	<u>0.74</u>
Casi NDVI + R2	0.15	0.30	0.58
Casi NDVI + R2 + R4	0.39	0.53	0.58
Casi NDVI + R1	0.17	0.31	0.59
Casi NDVI + R1 + R4	0.26	0.52	0.62
Red edge1	– 0.39	– 0.48	0.41
Red edge1 + R3	0.45	0.48	0.50
Red edge1 + R3 + R4	0.45	0.48	0.58
Carter 1	– 0.14	– 0.09	– 0.55
Carter 1 + R3	0.22	0.09	0.59
Carter 1 + R3 + R4	0.25	0.18	<u>0.72</u>
Carter 2	– 0.06	0.23	– 0.59
Carter 2 + R3	0.20	0.24	<u>0.64</u>
Carter 2 + R3 + R4	0.24	0.29	<u>0.75</u>
Botany	0.51	0.62	0.64
Botany + R3	0.55	0.64	0.62
Botany + R3 + R4	0.56	0.64	0.64
Geobotany	0.72	0.75	<u>0.79</u>
Geobotany + R3	<u>0.94</u>	<u>0.80</u>	<u>0.80</u>
Geobotany + R3 + R4	<u>0.96</u>	0.81	0.83
Enhanced geobotany	0.88	0.93	<u>0.99</u>
Enhanced geobotany + R3	<u>0.99</u>	0.93	<u>0.99</u>
Enhanced geobotany + R3 + R4	0.99	0.94	0.99

[a]Leaf Area Index; [b]canopy minus ambient temperature; [c]plant height; [d]number of data points used in the analysis; ND = not determined. R1 = Antenna pattern corrected SAR image; R2 = 3 × 3 pixel size Frost adaptive filtered SAR image; R3 = 11 × 11 pixel size Frost adaptive filtered SAR image; R4 = textural mean of SAR image. Correlation coefficients that are statistically significant at the 99% level are underlined.

The small-scale variations which are real and not attributable to speckle would be suppressed during filtering. While the scale of these variations was not directly measured during the field campaigns, it was noted during the ground-based data collection that the canola crops and one of the two pea fields exhibited the most visually apparent variations in LAI and plant height on the scale of a few metres or less. Perhaps not coincidentally these two crop types also exhibit decreases in correlation coefficients as the Frost filter size was increased.

The lack of systematic relationships complicates the task of specifying which operational parameters would be the most widely applicable. At the very least it would appear that the inclusion of SAR data in crop monitoring will result in increases in linear correlation coefficients. It also appears that tonal SAR data is as good as or better than textural data for crop condition monitoring. Beyond these general observations few systematic trends are apparent. The choice of using filtered or unfiltered SAR data cannot be specified in all cases; the linear correlation coefficients for optical + SAR data using either filtered or unfiltered SAR imagery can vary significantly. Ground-based observations may be required to determine whether small-scale variations in crop conditions exist. If such variations exist, unfiltered SAR imagery would probably be most appropriate. It is also possible that other unquantified field conditions such as small-scale variations in soil moisture or roughness may account for these variations.

The results of this campaign also suggest that inclusion of SAR textural data in the analysis may provide some modest benefits in some situations. It should be noted that in no cases did inclusion of the SAR textural mean data result in significant decreases in correlation coefficients.

The linear correlation coefficients for the individual radar 'bands' are also worth examining in greater detail. For the two crops for which statistically significant linear correlations were found, wheat and peas, LAI and plant height are inversely correlated with radar backscatter. This is at odds with simplified models of vegetation backscatter which imply a positive correlation (Ulaby *et al.* 1984, Brakke *et al.* 1981, Brisco and Brown 1990). Previous SAR agricultural studies did not explicitly measure LAI and hence the results of this study are not directly comparable with earlier work. Radar backscatter is sensitive to a number of factors in addition to above-ground biomass, factors such as soil moisture, row/field/ditch orientation and spacing, soil roughness, and crop phenology (e.g. Wu *et al.* 1985, Hutton and Brown 1986, Boivin *et al.* 1990, Bouman and van Kasteren 1990a, b). Any or all of these factors could be invoked to explain the observed relationships between the radar backscatter and plant parameters. During the field transects it was noted that row orientation, soil roughness and soil moisture were all quite variable within a single field.

As a general rule it is also found that linear correlation coefficients increase as the number of 'bands' of data used in the analysis increases (either optical or radar bands); hardly a surprising result. However it is worth considering these data in light of an operational environment. For digital imaging systems such as *casi*, the number of spectral bands of data that can be acquired is variable and depends upon operational parameters (Anger *et al.* 1994). The time and expense associated with digital data processing is not a simple linear function of the number of bands; the time required to process 13 bands of data is not 13 times as great as the time required to process one band of data. The results of this study suggest that improvements in correlation coefficients are correlated in some fashion with the number of bands of data; obviously there is an upper limit to this relationship.

Improvements in correlation coefficients may also be realized through other approaches. Some researchers have shown that improvements in correlation coefficients may be possible if the wavelength region used in the analysis is extended into the near and thermal infrared (Whitehead *et al.* 1986, Thenkabail *et al.* 1994). Improvements are also seen when narrow band passes, such as those used for this study, are applied rather than broad band passes (Demetriades-Shah *et al.* 1990, Stutte *et al.* 1990).

The results of this study suggest that some data sources may not need to be included in the analysis as they have little effect on correlation coefficients. The best example of this is the fact that SAR textural mean has no measurable effect on correlation coefficients for some crops, such as wheat. Some of the other general observations we have made above do not transcend all crop types and crop condition parameters. The decision whether to acquire and include both optical and SAR data in operational environments will probably be based on non-technical factors such as whether the increases in correlation justify the increased operational costs.

While it has been found that combined optical–SAR imagery will yield higher linear correlation coefficients than either sensor alone, the decision to use one or both sensors will be driven by a number of factors. These include the obvious considerations such as cost and sensor availability, but will also include other scientific and statistical issues. The most obvious of these is data accuracy. The level of accuracy and statistical significance required for a particular project may obviate the need for using combined optical + SAR data. Acceptable results may be obtained from either sensor alone. These are issues which are unique to a particular problem and the results of this study can be used as an indicator of the approximate levels of performance available from the different sensors.

7. Conclusions

This study was designed to investigate the applications of combined optical + SAR data to agricultural crop monitoring. The results indicate that the ability to monitor crop condition parameters such as LAI, canopy temperatures, and plant height are a function of crop type and field conditions. Other factors such as optical band passes, number of bands/images and image processing considerations (i.e. ratioing, filtering) will also have measurable effects on the derived linear correlation coefficients.

The results suggest that the inclusion of synthetic aperture radar data in the analysis will improve classification accuracies. The amount of improvement will depend on the type of radar image that is used in the analysis and there appears to be no easy way to predict *a priori* which radar 'band' will be most appropriate. Radar textural information also appears to be useful in some cases for increasing correlation coefficients.

The nature of the derived relationships between image and crop condition parameters suggests that, at least in this case, factors other than crop phenology may be affecting the radar backscatter. These factors may include soil moisture and surface roughness. Nevertheless the results indicate that combined optical + SAR imagery will yield greater linear correlation coefficients than either sensor alone.

Acknowledgements

This work was undertaken under the aegis of the National Research Council Industrial Research Assistance Program. The authors wish to thank Agriculture and Agri-food Canada, particularly Dr David Major, for technical assistance to the project, and Itres Research Ltd for providing the *casi* imaging system and for image geocorrection. Thanks also to Mr Ed Nikkel for generously providing access to his lands, and to Ian Major and Darren Nikkel for assisting with the ground campaigns. We also wish to thank the two anonymous reviewers for their thorough and insightful comments and suggestions.

References

Anger, C. D., Mah, S., and Babey, S. K., 1994, Technological enhancements to the Compact Airborne Spectrographic Imager (*casi*). *In Proceedings of the 1st International Airborne Remote Sensing Conference,* Vol. 2, *Strasbourg, France, 11–15 September* (Ann Arbor, MI: Environmental Research Institute of Michigan), pp. 205–213.

Banninger, C., 1989, Nature of the reflectance red edge in laboratory and FLI airborne imaging spectrometer data from a stressed coniferous forest. *In Image Processing '89; Sparks, Nevada* (Bethesda, MD: American Society for Photogrammetry and Remote Sensing), pp. 23–28.

Boivin, F., Gwyn, Q. H. J., and Thomson, K.P.B., 1990, Effets de la géométrie de surface de champs de mais sur la rétrodiffusion du radar bande C. *Canadian Journal of Remote Sensing*, **16,** 16–28.

Boochs, F., Kupfer, G., Dockter, K., and Kühbauch, W., 1990, Shape of the red edge as vitality indicator for plants. *International Journal of Remote Sensing*, **11,** 1741–1753.

Bouman, B. A. M., and van Kasteren, H. W. J., 1990a, Ground-based X-band (3-cm wave) radar backscattering of agricultural crops. I. Sugar beet and potato; backscattering and crop growth. *Remote Sensing of Environment*, **34,** 93–105.

Bouman, B. A. M., and van Kasteren, H. W. J., 1990b, Ground-based X-band (3-cm wave) radar backscattering of agricultural crops. II. Wheat, barley, and oats; the impact of canopy structure. *Remote Sensing of Environment*, **34,** 107–118.

Brakke, T. W., Kanemasu, E. T., Steiner, J. L., Ulaby, F. T., and Wilson, E., 1981, Microwave response to canopy moisture, leaf-area index, and dry weight of wheat, corn, and sorghum. *Remote Sensing of Environment*, **11,** 207–220.

Brisco, B., and Brown, R. J., 1990, Drought stress evaluation in agricultural crops using C-HH SAR data. *Canadian Journal of Remote Sensing*, **16,** 39–44.

Brisco, B., and Brown, R. J., 1995, Multidate SAR/TM synergism for crop classification in western Canada. *Photogrammetric Engineering and Remote Sensing*, **61,** 1009–1014.

Brisco, B., Brown, R. J., and Manore, M. J., 1989, Early season crop discrimination with combined SAR and TM data. *Canadian Journal of Remote Sensing*, **15,** 44–54.

Brown, R. J., Manore, M. J., and Poirier, S., 1992, Correlations between X-, C-, and L-band imagery within an agricultural environment. *International Journal of Remote Sensing*, **13,** 1645–1661.

Carter, G. A., 1993, Responses of leaf spectral reflectance to plant stress. *American Journal of Botany*, **80,** 239–243.

Carter, G. A., 1994, Ratios of leaf reflectances in narrow wavebands as indicators of plant stress. *International Journal of Remote Sensing*, **15,** 697–703.

Carter, G. A., and Miller, R. L., 1994, Early detection of plant stress by digital imaging within narrow stress-sensitive wavebands. *Remote Sensing of Environment*, **50,** 295–302.

Carter, G. A., Mitchell, R. J., Chappelka, A. H., and Brewer, C. H., 1992, Response of leaf spectral reflectance in loblolly pine to increased atmospheric ozone and precipitation acidity. *Journal of Experimental Biology*, **43,** 577–584.

Cloutis, E. A., Connery, D. R., Major, D. J., and Dover, F. J., 1996a, Airborne multispectral monitoring of agricultural crop status: effect of time of year, crop type and crop condition parameter. *International Journal of Remote Sensing*, **17,** 2579–2601.

Cloutis, E. A., Connery, D. R., Major, D. J., and Dover, F. J., 1996b, Agricultural crop condition monitoring using airborne C-band synthetic aperture radar in southern Alberta. *International Journal of Remote Sensing*, **17,** 2565–2577.

Cohen, W. B., 1991, Temporal versus spatial variation in leaf reflectance under changing water stress conditions. *International Journal of Remote Sensing*, **12,** 1865–1876.

Daughtry, C. S. T., Ranson, K. J., and Biehl, L.L., 1991, C-band backscattering from corn canopies. *International Journal of Remote Sensing*, **12,** 1097–1109.

Davis, J. C., 1986, *Statistics and Data Analysis in Geology*, 2nd edn (New York: Wiley).

Demetriades-Shah, T. H., Steven, M. D., and Clark, J.A., 1990, High resolution derivative spectra in remote sensing. *Remote Sensing of Environment*, **33,** 55–64.

Dixon, R., and Mack, A., 1991, Crop discrimination in the Carberry area with combined SAR and TM data. *In Proceedings of the 14th Canadian Symposium on Remote Sensing, Calgary, Alberta, 6–10 May 1991* (Ottawa: Canadian Remote Sensing Society), pp. 118–123.

Fernández, S., Vidal, D., Simón, E., and Solé-Sugrañes, E., 1994, Radiometric characteristics of *Triticum aestivum* cv. Astral under water and nitrogen stress. *International Journal of Remote Sensing*, **15,** 1867–1884.

Fischer, J. A., Brown, R. J., and Brisco, B., 1992, The effects of changes in soil moisture and rainfall on SAR data crop classification. *In Proceedings of the 15th Canadian Symposium on Remote Sensing, Toronto, Ontario, 1–4 June 1992* (North York: Ontario Centre for Remote Sensing), pp. 221–226.

Foody, G. M., McCulloch, M. B., and Yates, W. B., 1994, Crop classification from C-band polarimetric radar data. *International Journal of Remote Sensing*, **15,** 2871–2885.

Hutton, C. A., and Brown, R. J., 1986, Comparison of space and airborne L-HH radar imagery in an agricultural environment. *In Proceedings of the 10th Canadian Symposium on Remote Sensing, Edmonton, Alberta, 5–8 May 1986* (Ottawa: Canadian Aeronautics and Space Institute), pp. 171–181.

Livingstone, C. E., Gray, A. C., Hawkins, R. K., Olsen, J. G., and Halbertsman, J. G., 1987, C-band radar: system description and test results. *In Proceedings of the 11th Canadian Symposium on Remote Sensing, Waterloo, Ontario, 22-25 June 1987* (Ottawa: Canadian Aeronautics and Space Institute), pp. 503-518.

Major, D. J., Brisco, B., and Brown, R. J., 1991, Seasonal trajectory of radar backscatter of wheat and canola canopies. *In Proceedings of the 14th Canadian Symposium on Remote Sensing, Calgary, Alberta, 6–10 May 1991* (Ottawa: Canadian Remote Sensing Society), pp. 448–451.

Major, D. J., Larney, F. J., Brisco, B., Lindwall, C. W., and Brown, R. J., 1993, Tillage effects on radar backscatter in southern Alberta. *Canadian Journal of Remote Sensing*, **19,** 170–176.

Malthus, T. J., and Madeira, A. C., 1993, High resolution spectroradiometry: Spectral reflectance of field bean leaves infected by *Botrytis fabea*. *Remote Sensing of Environment*, **45,** 107–116.

Miller, J. R., Hare, E. W., and Wu, J., 1990, Quantitative characterization of the vegetation red edge reflectance, 1. An inverted-Gaussian reflectance model. *International Journal of Remote Sensing*, **11,** 1755–1773.

Paris, J. F., and Kwong, H. H., 1988, Characterization of vegetation with combined thematic mapper (TM) and shuttle imaging radar (SIR-B) image data. *Photogrammetric Engineering and Remote Sensing*, **54,** 1187–1193.

PCI (1992) *Using PCI Software* (Richmond Hill, Ontario: PCI Ltd).

Peñuelas, J., Gamon, J. A., Fredeen, A. L., Merino, J., and Field, C. B., 1994, Reflectance indices associated with physiological changes in nitrogen- and water-limited sunflower leaves. *Remote Sensing of Environment*, **48,** 135–146.

Prevot, L., Dechambre, M., Taconet, O., Vidal-Madjar, D., Normand, M., and Galle, S., 1993, Estimating the characteristics of vegetation canopies with airborne radar measurements. *International Journal of Remote Sensing*, **14,** 2803–2818.

Pultz, T. J., and Brown, R. J., 1987, SAR image classification of agricultural targets using first- and second-order statistics. *Canadian Journal of Remote Sensing*, **13,** 85–91.

Pultz, T. J., Leconte, R., Brown, R. J., and Brisco, B., 1990, Quantitative soil moisture extraction from airborne SAR data. *Canadian Journal of Remote Sensing*, **16,** 59–62.

Railyan, V. Y., and Korobov, R. M., 1993, Red edge structure of canopy reflectance spectra of triticale. *Remote Sensing of Environment*, **46,** 173–182.

Smith, A. M., Major, D. J., Lindwall, C. W., and Brown, R. J., 1995, Multi-temporal, multi-sensor remote sensing for monitoring soil conservation farming. *Canadian Journal of Remote Sensing*, **21,** 177–184.

Stutte, G. W., Bors, R., and Stutte, C. A., 1990, Quantification of nutrient stress in horticultural crops using videography. *Journal of Imaging Technology*, **16,** 104–107.

Thenkabail, P. S., Ward, A. D., Lyon, J. G., and Merry, C. J., 1994, Thematic mapper vegetation indices for determining soybean and corn growth parameters. *Photogrammetric Engineering and Remote Sensing*, **60,** 437–442.

Thomson, K. P. B., Edwards, G., Landry, R., Jaton, A., Cadieux, S. P., and Gwyn, Q. H. J., 1990, SAR applications in agriculture: multiband correlation and segmentation. *Canadian Journal of Remote Sensing*, **16,** 47–54.

Tingle, J., and Stoll, J., 1990, Spectral sensing of crops for monitoring physiological stress. *In Proceedings of the US Army Corps of Engineers 7th Remote Sensing Symposium held in Portland, Oregon, 7–9 May 1990* (Washington, DC: US Army Corps of Engineers), pp. 462–481.

Treitz, P. M., Barber, D. G., and Howarth, P. J., 1991, Texture measures for the discrimination of agricultural crops in southwestern Ontario. *In Proceedings of the 14th Canadian Symposium on Remote Sensing, Calgary, Alberta, 6–10 May 1991* (Ottawa: Canadian Remote Sensing Society), pp. 224–227.

Ulaby, F. T., and Wilson, E. A., 1985, Microwave attenuation properties of vegetation canopies. *IEEE Transactions on Geoscience and Remote Sensing*, **23,** 746–753.

Ulaby, F. T., Allen, C. T., Eger, G., and Kanemasu, E., 1984, Relating the microwave backscattering coefficient to leaf area index. *Remote Sensing of Environment*, **14,** 113–133.

Wallace, J. F., Campbell, N. A. S., Wheaton, G. A., and McFarlane, D. J., 1993, Spectral discrimination and mapping of waterlogged cereal crops in Western Australia, *International Journal of Remote Sensing*, **14,** 2731–2743.

Whitehead, V. S., Johnson, W. R., and Boatwright, J. A., 1986, Vegetation assessment using a combination of visible, near-IR, and thermal-IR AVHRR data. *IEEE Transactions on Geoscience and Remote Sensing*, **24,** 107–112.

Wu, L. K., Moore, R. K., and Zoughi, R., 1985, Sources of scattering from vegetation canopies at 10 GHz. *IEEE Transactions on Geoscience and Remote Sensing*, **23,** 737–745.